Future Engineering Research

Open Access Journal

November 2026| Volume 01 | Issue 01 | Pages 10-18

Journal homepage: https://fupubco.com/fer

https://doi.org/10.55670/fpll.fer.1.1.2

Future Publishing LLC

Article

Numerical simulation and control measures for deflagration in ventilation ducts of polyimide foam production line

Yiting Li, Liang Jiang, Zhangsheng Yin, Mingchao Yin, Tianyu Guo, Donglin Yang, Xiaohong Gui*

China University of Mining & Technology, Beijing, Beijing 100083, China

* Corresponding Author: gxhbox@sina.com

ABSTRACT

Polyimide foam exhibits excellent high-temperature resistance, flame retardancy, and sound absorption performance, and is widely used in aerospace, advanced equipment, and other high-tech fields. However, its production process involves inherent deflagration risks from combustible dust and volatile organic gases. Using the ventilation and dust-collection duct of a polyimide foam production line as the research object, this paper establishes a numerical deflagration model in ANSYS Fluent to investigate the propagation behavior of gas-dust mixtures inside the duct. The evolution characteristics of velocity, temperature, pressure, species distribution, and particle motion are systematically analyzed. Quantitative results show that the peak gas temperature in the main reaction zone reaches approximately 1680 K, the maximum local flow velocity is 24.3 m/s, and the minimum gas density drops to 0.20–0.40 kg/m³. The middle horizontal section of the duct is identified as the primary deflagration zone, while elbows and areas with structural discontinuities are high-risk locations with significant pressure concentration and flow turbulence. Based on this, targeted risk control measures are proposed, including duct structure optimization, explosion venting and isolation arrangement, dust concentration management, online monitoring system construction, and ignition source control. This study provides theoretical support for explosion-proof design and safety optimization of ventilation and dust removal systems in polyimide foam production lines.

Keywords: *Polyimide, Deflagration, Numerical simulation, Risk management and control*

Received: 10 July 2026 Received in revised form: 02 September 2026 Accepted: 16 September 2026

DOI: 10.55670/fpll.fer.1.1.2

1. INTRODUCTION

Electric Polyimide foam is a porous material mainly composed of polyimide resin, with multi-scale open-cell, closed-cell, or composite cell structures. Its density is customizable from 5–400 kg/m³, and it offers outstanding insulation performance. With excellent high- and low-temperature resistance, radiation resistance, sound absorption, flame retardancy, low smoke emission, and low toxic gas release, polyimide foam can serve as thermal insulation, sound absorption, or flame-retardant materials, as well as supports and sandwich layers for advanced composite materials [1-4]. It has been widely applied in critical scenarios such as thermal insulation, interlayer structures, sound absorption, shock protection, and electrical insulation in high-tech sectors including aerospace, national defense equipment, high-end buildings, and microelectronics [5]. With the increasing demand for high-performance composite materials, polyimide foam materials are gradually developing towards large-scale industrial production [6,7]. The production of polyimide foam faces multiple safety challenges. First, the mixed resin in raw materials contains methanol and tetrahydrofuran, which are Class A fire hazardous substances with significant deflagration risks [8]. Second, polyimide resin powder presents a high dust explosion risk: dust clouds are highly ignitable and exhibit high explosion severity and rapid propagation velocity. During operation, combustible gases and dust may form explosive mixtures in confined spaces. Once exposed to ignition sources such as electrostatic sparks, high-temperature surfaces, or mechanical friction, fire or deflagration accidents are highly likely to occur [9]. Previous studies on polyimide foam have mainly focused on material preparation processes, performance optimization, and application expansion [10-14]. In contrast, research on safety risks, especially deflagration hazards during production and propagation laws in ventilation and dust collection ducts, remains relatively limited. Existing work lacks systematic analysis of the coupling behaviors of combustible medium flow, temperature field evolution, and pressure wave propagation in complex ducts, and thus fails to provide effective theoretical support for explosion-proof design and safety optimization of polyimide foam production lines.

With the development of computational fluid dynamics (CFD) technology, numerical simulation methods have been widely applied in fire and deflagration propagation research [15]. Through mathematical modeling, researchers can accurately simulate temperature fields, pressure fields, and hazardous area distribution during deflagration, providing an important approach to risk analysis of complex industrial systems. Therefore, this paper takes the ventilation and dust collection duct of a polyimide foam production line as the research object and establishes a duct deflagration model using Fluent to simulate and analyze the propagation of combustible media inside the duct. Using velocity, temperature, pressure, species distribution, and particle-motion characteristics, the study examines how elbows and structural changes affect deflagration behavior and identifies potentially hazardous areas in the system. The study further proposes corresponding explosion-proof optimization and safety control measures, aiming to provide a theoretical reference for the safety design and risk prevention of ventilation and dust removal systems in polyimide foam production lines.

2. MATHEMATICAL MODEL FOR DUCT DEFLAGRATION

The deflagration in the ventilation duct of a polyimide foam production line is a complex physical and chemical process involving the coupling of gas-phase combustion and dust particles. Before simulation, we make reasonable simplifications to describe the combustion and deflagration of the gas-dust-air multiphase system and to numerically calculate key variations in the flow field, temperature field, pressure field, and species concentration during deflagration. The mathematical model is established based on the following assumptions:

- All gas-phase components are treated as ideal gases;
- The deflagration is a transient process, and radiative heat transfer is neglected;
- Body forces affecting flow and particle motion are not considered;
- The combustion reaction is simplified as a single-step irreversible reaction;
- The specific heat capacity of mixed gases follows the mixing rule;
- The Soret effect and Dufour effect are ignored;
- Duct walls are rigid stationary no-slip walls, and wall displacement and deformation are excluded.

2.1 Governing equations

In this study, the actual three-dimensional duct is simplified to a two-dimensional plane flow and deflagration problem. An unsteady method is adopted to simulate the transient deflagration process, corresponding to unsteady flow in a two-dimensional Cartesian coordinate system. The governing equations include the continuity, momentum, energy, and species transport equations [16,17].

Continuity equation

$$\frac{\partial \rho}{\partial t}+\frac{\partial}{\partial x}(\rho v_x)+\frac{\partial}{\partial y}(\rho v_y)=0 \tag{1}$$

Momentum equation

$$\frac{\partial(\rho v_x)}{\partial t}+\frac{\partial(\rho v_x^2)}{\partial x}+\frac{\partial(\rho v_x v_y)}{\partial y}=-\frac{\partial P}{\partial x}+\frac{\partial S_{xx}}{\partial x}+\frac{\partial S_{xy}}{\partial y} \tag{2}$$

Energy equation

$$\frac{\partial(\rho E)}{\partial t}+\frac{\partial(\rho E v_y)}{\partial y}+\frac{\partial(\rho v_x E)}{\partial x}=-\frac{\partial P v_y}{\partial y}+\frac{\partial(S_{yy}v_y)}{\partial y}+\frac{\partial(S_{xy}v_x)}{\partial y}-\frac{\partial(P v_x)}{\partial x}+\frac{\partial(S_{xx}v_x)}{\partial x}+\frac{\partial(S_{xy}v_y)}{\partial y} \tag{3}$$

Species equation

$$\frac{\partial(\rho Y_i)}{\partial t}+\frac{\partial}{\partial x}(\rho v Y_i-\frac{\mu_e}{\sigma_i}\frac{\partial Y_i}{\partial x})-R_i=0 \tag{4}$$

where ρ is the fluid density (kg·m^{-3}); v_x and v_y are the velocity components in the x and y directions (m·s^{-1}) , respectively; P is pressure (Pa); E is internal energy (J); S_{xx} ,S_{yy} and S_{xy} are components of the viscous deviatoric stress tensor (Pa); Y_i is the mass fraction of the i-th component; R_i is the chemical reaction generation/consumption rate (kmol·m^{-3}·s^{-1}); μ_e is the dynamic viscosity coefficient (kg·m^{-1}·s^{-1}); σ_i is an empirical constant.

2.2 Turbulence model

High-speed flow and intense disturbances occur during deflagration, and the flow field shows clear turbulent characteristics. To accurately describe the turbulent behavior during deflagration propagation, the standard k-ε turbulence model is adopted for flow field solution in this study**Error! Reference source not found.**.Standard wall functions are used to treat the near-wall region, which matches the flow characteristics of industrial ventilation ducts.

Transport equation for turbulent kinetic energy k:

$$\frac{\partial(\rho k)}{\partial t}+\frac{\partial(\rho k u_i)}{\partial x_i}=\frac{\partial}{\partial x_j}[(\mu+\frac{\mu_t}{\sigma_k})\frac{\partial k}{\partial x_j}]+G_k+G_b-\rho\varepsilon-Y_M \tag{5}$$

Transport equation for turbulent dissipation rate $\mathcal{E}$:

$$\frac{\partial(\rho\varepsilon)}{\partial t}+\frac{\partial(\rho\varepsilon u_i)}{\partial x_i}=\frac{\partial}{\partial x_j}[(\mu+\frac{\mu_t}{\sigma_\varepsilon})\frac{\partial\varepsilon}{\partial x_j}]+C_{1\varepsilon}\frac{\varepsilon}{k}(G_k+C_{2\varepsilon}G_b)-C_{2\varepsilon}\rho\frac{\varepsilon^2}{k} \tag{6}$$

where G_k is the turbulent kinetic energy generated by the velocity gradient; G_b is the turbulent kinetic energy generated by buoyancy; Y_M represents the dilatation term of compressible turbulent fluctuation; μ_t is the turbulent viscosity; $C_{1\varepsilon}$, $C_{2\varepsilon}$ and $C_{2\varepsilon}$ are empirical constants with typical values of 1.44, 1.92, and 0.80, respectively.

The standard k-ε turbulence model is stable and applicable in engineering practice, and it can effectively simulate flow characteristics in elbow sections, high-speed regions, and local vortex areas during deflagration.

2.3 Combustion model and reaction rate model

The deflagration reaction mechanism of the polyimide dust-methanol gas mixture is complex. To balance computational accuracy and efficiency, the reaction is simplified to a single-step irreversible reaction, and the

Species Transport Model is applied. This model solves the transport and diffusion behavior of multiple chemical components simultaneously and effectively simulates the mixing, transport, and reaction processes of each component. For turbulence-chemistry interaction, the Eddy-Dissipation model is selected, which assumes that turbulent mixing controls the reaction rate. This model is widely used in deflagration simulations with fast chemical reaction rates, and can well describe the coupling between turbulent flow and combustion. The simulation enables the diffusion energy source term to ensure energy conservation for multicomponent diffusion. The governing equation of species transport is as follows [18]:

$$\frac{\partial(\rho Y_i)}{\partial t} + \nabla(\rho v Y_i) = -\nabla J_i + R_i + S_i \tag{7}$$

where *Yi* is the mass fraction of each component; *Ri* is the net production rate of components ($kmol\cdot m^{-3}\cdot s^{-1}$); *Si* is the additional source term of components （$kmol\cdot m^{-3}\cdot s^{-1}$).

Stoichiometric equation: The gas-phase oxidation of methanol is simplified as a single-step irreversible volumetric reaction, with the stoichiometric equation:

$$2CH_3OH + 3O_2 \rightarrow 2CO_2 + 4H_2O \tag{8}$$

Reaction rate parameters: In the Eddy-Dissipation model, the reaction rate is determined by the turbulent mixing time scale, and the mixing rate constants are set as:
Arrhenius pre-exponential factor: $A = 1.0 \times 10^{15}$
Activation energy: $E_a = 100J/kgmol$
Temperature exponent: $n = 0$
Eddy-Dissipation model constants: A=4, B=0.5

2.4 Discrete phase model and interphase coupling

The gas-particle two-phase flow in the duct is simulated under the Eulerian-Lagrangian framework. The gas phase is solved as a continuous medium by the Eulerian method, and polyimide dust particles are tracked as the discrete phase by the Lagrangian Discrete Phase Model (DPM). Since the volume fraction of dust in the ventilation duct is far below 10%, the flow belongs to the dilute flow regime, which is within the application scope of the DPM model.

Drag law: The Schiller-Naumann drag model is used to calculate the drag force on particles, which is applicable to spherical particles in a wide range of particle Reynolds number ($Re_p \leq 1000$) . The drag coefficient C_d is defined as:

$$C_d = \begin{cases} \frac{24}{Re_p}(1 + 0.15Re_p^{0.687}) & Re_p \leq 1000 \\ 0.44 & Re_p > 1000 \end{cases} \tag{9}$$

The momentum exchange between gas and particles is added to the gas-phase momentum equation as a momentum source term to realize two-way momentum coupling.

Interphase heat transfer: The Ranz-Marshall convective heat transfer correlation is adopted to describe the heat exchange between gas and particles:

$$Nu = 2.0 + 0.6Re_p^{1/2}Pr^{1/3} \tag{10}$$

where Nu is the Nusselt number, and Pr is the Prandtl number of the gas phase. The heat transfer between particles and gas is fed back to the gas-phase energy equation as an energy source term.

In this simulation, the chemical reaction is dominated by gas-phase methanol oxidation. Polyimide dust particles participate in the deflagration process mainly through interphase momentum and energy coupling, which enhances turbulent mixing and heat transfer, and promotes the development of the combustion reaction.

2.5 Justification of modeling simplifications

Several simplifications are adopted in the numerical model, and their rationales are elaborated as follows to support the reliability of the simulation results. The primary objective of this study is to reveal the overall propagation law of gas-dust deflagration in the duct and identify the relative distribution of hazardous zones, rather than to precisely quantify three-dimensional local flow details. For long ventilation ducts where axial and radial variations dominate the deflagration process, similar CFD studies on duct deflagration [19] widely adopt a two-dimensional plane simplification, which can effectively capture the main characteristics of temperature, pressure, and flow fields. This simplification significantly reduces computational cost while retaining the core physical mechanism of deflagration propagation, and is sufficient to identify high-risk areas and propose safety control measures in this work. Under the simulated conditions, the dust loading is low, and the main gas components are diatomic gases (N_2, O_2) with weak radiative properties. The volume fractions of radiative gases (CO_2, H_2O) generated by the reaction are limited in the main flow region. Because this study focuses on identifying hazardous areas and ranking relative risk rather than precisely predicting extreme accident conditions, neglecting radiative heat transfer is acceptable.

2.6 Limitations

To ensure scientific transparency and clarify the scope of the research conclusions, this section systematically discusses the potential impacts of major modeling simplifications on the identified hazardous zones. First, the combustion reaction is simplified as a single-step irreversible global reaction. This treatment omits intermediate reaction pathways and radical species, which may introduce deviations in the precise prediction of reaction rate and peak temperature. However, since this study focuses on identifying the relative distribution of hazardous zones rather than quantifying extreme reaction parameters, the spatial location of the primary deflagration zone and the overall consumption trend of combustible components remain reliable. Second, the three-dimensional duct is simplified to a two-dimensional plane flow model. Three-dimensional secondary flow effects at elbows and structural discontinuities are not fully captured, which may cause slight deviations in local peak velocity and pressure values. Nevertheless, the axial propagation law of deflagration and the relative risk ranking of different duct sections are consistent with the physical process, and the core conclusion that elbows are high-risk areas of pressure concentration remains valid. Third, the simulation neglects radiative heat transfer. Under the high-temperature conditions of deflagration, thermal radiation contributes to heat dissipation. Ignoring radiation may slightly overestimate the local peak temperature, but it has limited influence on the spatial extent of high-temperature zones and the location of the main reaction zone. For hazard zone identification and relative risk assessment, this simplification does not change the fundamental distribution of hazardous areas. Fourth, we treat the duct walls as rigid, stationary, no-slip walls with no heat conduction loss. In actual engineering scenarios, heat transfer through duct walls will reduce the overall temperature to some extent but will not change the structural effect of pressure-wave reflection and superposition at elbows. This assumption does not affect the identification of key hazardous areas dominated by geometric structure. Overall, these simplifications may cause quantitative deviations in extreme parameters such as peak temperature and maximum overpressure, but will not alter the qualitative distribution of hazardous zones. The core conclusions of this study on the location of primary reaction zones and key hazardous areas are robust.

3. NUMERICAL SIMULATION OF POLYIMIDE DEFLAGRATION

To further explore the deflagration behavior and risk evolution law of polyimide dust under typical process conditions, the CFD method is adopted to conduct numerical simulation of dust deflagration in the high-risk ventilation and dust collection duct system of the production line. By establishing a geometric model and setting multiphase flow and chemical reaction mechanisms, the variation characteristics of the velocity field, temperature field, pressure field, species concentration field, and particle phase behavior inside the duct under the coexistence of combustible gas, oxygen, and polyimide dust are systematically simulated and analyzed.

3.1 Geometric model

The duct geometric model (Figure 1) is established based on actual production processes. While retaining the main characteristics of flow and deflagration propagation, the complex actual duct structure is simplified to reduce computational cost and improve numerical convergence efficiency. The geometric model was built in SpaceClaim. The overall model is L-shaped, consisting of an inlet section, a 90° elbow connecting section, a horizontal straight conveying section, and an outlet section, which is basically consistent with the actual ventilation and dust removal system. Multiphase flow containing polyimide dust and combustible gas enters from the right inlet, turns through the 90° elbow, and finally discharges from the left outlet. The model is approximately 65 m long, and the main duct width is 0.8 m. The model includes 90° circular-arc elbows and local cross-section discontinuity structures to simulate connecting parts and local disturbance areas in actual industrial ducts.

Figure 1. Geometric structure of ventilation duct

Fluent Meshing is used for mesh generation (Figure 2). Given the complexity of the combustion and deflagration process, fine meshes are used to accurately capture the temperature field, pressure field, and shock-wave propagation during deflagration. To balance computational accuracy and runtime, we use quadrilateral meshes with a unit size of 50 mm. Local mesh refinement is implemented in elbow areas and structural discontinuity zones to better capture complex flow fields and deflagration propagation.

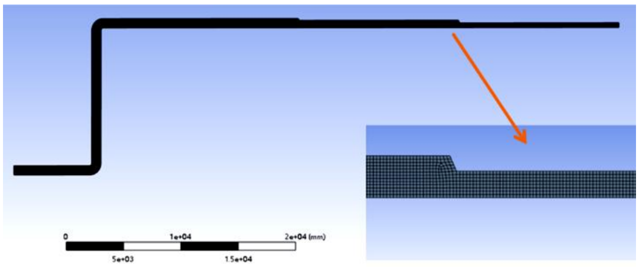

Figure 2. Schematic diagram of mesh generation

3.2 Boundary conditions

The computational domain includes two velocity inlets, one pressure outlet, and wall boundaries.

Inlet boundaries:

Air inlet: Velocity inlet condition, velocity magnitude = 13 m/s, perpendicular to the boundary; Turbulent kinetic energy k = 3.79 m^2/s^2, turbulent dissipation rate ε=539m^2/s^2.

Dust-methanol inlet: Velocity inlet condition, velocity magnitude = 13 m/s, perpendicular to the boundary; Turbulent kinetic energy k = 0.53m^2/s^2, turbulent dissipation rate ε = 18.4m^2/s^2; Gas-phase component: methanol mass fraction = 0.9; Polyimide dust: mass loading = 0.05 kg/m^3, particle size follows Rosin-Rammler distribution with median diameter d_{50}=45 μm and distribution index n=1.8.

Outlet boundary: A pressure outlet condition is adopted with gauge pressure = 0 Pa. The backflow turbulence intensity is set to 5% and the turbulence viscosity ratio is 5.

Wall boundary: All duct walls are set as stationary no-slip walls with standard wall functions. The wall temperature is constant at 300 K, and the wall roughness height is 0 m. The initial temperature of the computational domain is 300 K, and the initial pressure is 101.325 kPa.

3.3 Analysis of simulation results

Temperature field: The overall temperature contour shows that the temperature field inside the ventilation and dust collection duct presents obvious axial and local inhomogeneity (Figure 3). Gas flows horizontally from the right inlet and exits from the lower-left outlet. In the inlet section and adjacent straight pipe areas, the overall temperature is relatively low and uniformly distributed, with no obvious local high-temperature accumulation, indicating that no intense reaction or energy release occurs in these regions. Obvious local high-temperature zones appear in the middle horizontal section of the duct, where the temperature reaches its peak value. These band-shaped high-temperature zones form distinct temperature gradients near the duct walls. This phenomenon indicates that intense exothermic reactions occur in the system; combustible components, including methanol vapor and polyimide dust particles, undergo rapid oxidation in the presence of oxygen, and local areas have entered the deflagration stage. The temperature gradually decreases as the gas flows towards the lower-left outlet, indicating that the high-temperature reaction zones are mainly concentrated in the middle pipe section. In downstream areas, the reaction intensity declines significantly, dominated by the flow of high-temperature products and heat diffusion. In summary, the local high-temperature zones in the middle horizontal pipe section are identified as potential deflagration areas. These regions satisfy one of the key conditions for dust explosions (concentrated high-temperature heat sources) and should be regarded as key areas for subsequent risk control and structural reinforcement.

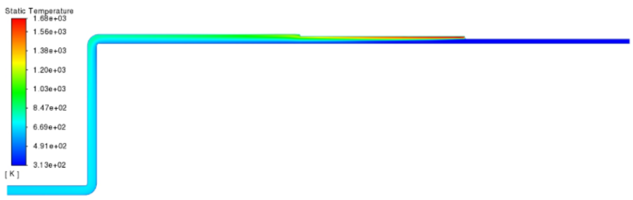

Figure 3. Overall temperature distribution

Pressure field: The overall absolute pressure inside the duct is close to ambient pressure, yet clear pressure concentrations and gradient changes occur in local areas, especially at duct elbows (Figure 4). Pressure is relatively uniform in straight pipe sections and changes gently along the flow direction, indicating that flow and reactions have limited influence on pressure in areas with stable geometry. In contrast, local pressure at duct elbows is significantly higher than in adjacent straight pipes, forming typical pressure-concentration zones. This phenomenon results from three combined factors: (1) high-temperature gas generated by deflagration is constrained by geometric structures at elbows; (2) flow direction reversal leads to momentum redistribution and local gas compression; (3) pressure waves reflect and superpose at elbows, increasing the instantaneous local pressure.

Although the absolute pressure rise is limited under the current simulation condition, the pressure concentration phenomenon confirms that elbow areas are highly sensitive to pressure disturbances induced by deflagration. Under adverse working conditions such as higher dust concentration, local confinement, or secondary ignition, these areas are prone to forming dangerous overpressure peaks. The pressure gradually attenuates as it propagates downstream through the elbows, indicating that the duct structure can dissipate and buffer pressure waves to a certain extent. Meanwhile, elbows bear the primary impact of pressure waves during deflagration. From a safety perspective, the geometric discontinuity makes duct elbows structurally weak and vulnerable to pressure concentration during deflagration. Therefore, elbows are key protective components of the ventilation and dust removal system, and their explosion resistance, explosion-proof structures, and pressure-relief measures should be prioritized in subsequent safety design.

Velocity field: The overall velocity contour reflects the flow field structure and turbulent characteristics inside the duct, which is crucial for judging deflagration propagation risks (Figure 5). After entering from the right inlet, the gas quickly forms a stable flow field with uniform velocity distribution in straight pipe sections. The flow velocity rises markedly at elbows and other areas of local geometric variation, with a maximum local velocity of 22–24 m/s. Three flow characteristics are observed in these areas: (1) local flow acceleration caused by curved streamlines; (2) enhanced shear effect and significantly increased turbulence intensity; (3) easy re-suspension and local enrichment of dust particles.

Notably, the high-velocity areas overlap with or adjoin the aforementioned high-temperature zones. High-speed gas flow not only improves the mixing efficiency of combustible dust and oxygen, but also accelerates flame propagation and intensifies combustion. In summary, the high-velocity flow and strong turbulent environment in the middle pipe section provide favorable dynamic conditions for dust deflagration. Once ignition or local thermal runaway occurs, rapid deflagration will easily propagate upstream and downstream along the duct.

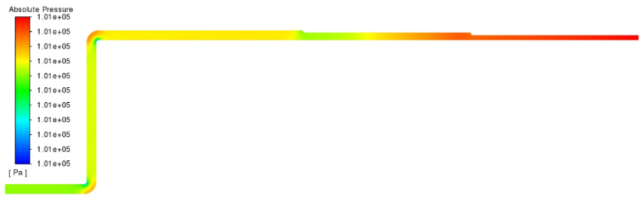

Figure 4. Overall pressure distribution

Figure 5. Overall velocity distribution

Density field: The overall density contour reflects the thermal expansion and compression of a multi-component mixed gas during deflagration, helping identify reaction intensity and flow state (Figure 6). The density distribution inside the duct is significantly inhomogeneous and varies remarkably along the flow direction from the right inlet to the lower-left outlet. At the right inlet and adjacent areas, the density is relatively high at approximately 1.1–1.2 kg/m^3 with a uniform distribution, close to the gas density under normal temperature and pressure. It indicates that no intense chemical reaction or obvious thermal expansion occurs in these regions, and the flow state remains stable. Distinct low-density zones exist in the middle horizontal pipe section, where the minimum density drops to 0.2–0.4 kg/m^3. These low-density zones are highly consistent with the high-temperature zones in the temperature contour. This spatial correspondence indicates that: (1) intense exothermic reactions lead to a sharp rise in gas temperature; (2) severe gas thermal expansion reduces the mass per unit volume; (3) obvious reaction-induced expansion occurs in these areas.

Gas density gradually recovers as the fluid flows downstream and toward the outlet, meaning the high-temperature post-reaction gas cools gradually during flow and mixing, and density tends to remain stable. Significant

density reduction is typical during deflagration. The emergence of low-density zones reflects intense energy release and gas expansion in local areas, and also creates favorable conditions for the propagation of pressure waves and flames.

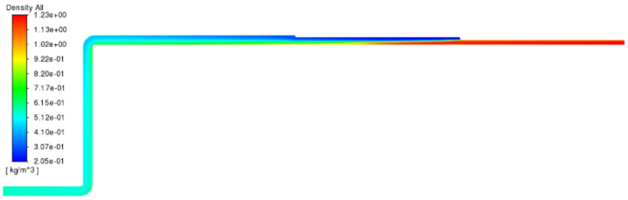

Figure 6. Overall density distribution

Species distribution: A comprehensive analysis of the mass-fraction distribution of each component further clarifies the location and intensity of chemical reactions inside the duct. Figure 7 shows the contours of mass fraction distribution for methanol, CO_2, and O_2. In the inlet and upstream areas, the mass fractions of methanol and oxygen are relatively high and distributed continuously in the straight pipe sections, while the CO_2 concentration is low. This shows that no obvious reaction occurs in these regions. In the middle horizontal pipe section, the mass fraction of methanol decreases sharply, overlapping with the low-oxygen zones formed by rapid oxygen consumption and the high-concentration CO_2 zones. This indicates that oxygen is rapidly consumed for the oxidation reaction of methanol and dust particles in this section. Further downstream, methanol and oxygen concentrations continue to decrease and stabilize, and CO_2 concentration also tends to remain constant. The results show that reactions are mainly concentrated in the middle pipe section, and downstream areas are dominated by the flow of reaction products.

Particle motion characteristics: Particle temperature is an important indicator to judge whether dust participates in or intensifies combustion reactions. Figure 8 shows the particle temperature distribution. The particle temperature distribution shows that the temperature of dust particles rises significantly in the middle horizontal pipe section, and the maximum particle temperature is basically consistent with that of the gas phase. This indicates that dust particles are in close contact with the high-temperature gas, undergo significant heating, and even participate in oxidation reactions, acting as important carriers of heat transfer and energy release. The high-temperature particle zones coincide with the consumption zones of methanol and oxygen and the generation zones of CO_2, further confirming that this section is the main reaction area.

The particle pressure distribution reflects the mechanical environment of dust particles during flow and reactions. Figure 9 shows the particle pressure distribution. Overall, particle pressure follows the gas-phase pressure and changes gently in straight pipe sections. However, particle pressure rises markedly at duct elbows and forms local pressure-concentration zones. The reasons are as follows: (1) flow restriction at elbows hinders particle movement; (2) gas-phase pressure waves act on particles and generate additional stress; (3) particles bear impact loads and local structural effects in these areas. This result is fully consistent with the gas-phase pressure analysis, showing that duct elbows are subjected to coupled gas- and particle-phase pressure under deflagration conditions, so their structural safety is critical.

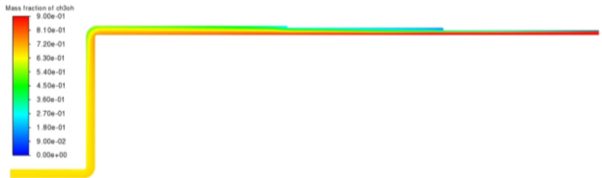

(a) CH_3OH distribution

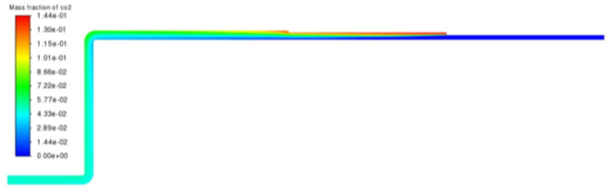

(b) CO_2 distribution

(c) O_2 distribution

Figure 7. Contours of species mass fraction distribution

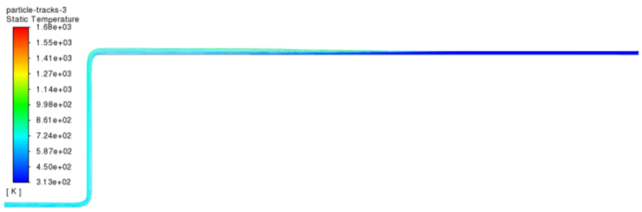

Figure 8. Particle temperature distribution

Figure 9. Particle pressure distribution

The particle velocity distribution reveals the motion characteristics of polyimide dust in the ventilation and dust collection duct and its coupling relationship with the gas-phase flow field. Figure 10 shows the particle velocity distribution. The overall particle velocity distribution is consistent with the gas-phase velocity, showing that gas-phase drag mainly controls dust-particle motion and that the particles exhibit clear flow-following characteristics. The particle velocity is uniformly distributed in straight pipe sections, while it increases with larger velocity gradients at elbows. Flow-direction reversal changes particle trajectories; enhanced local turbulence intensifies relative particle motion and increases collision probability, which can easily cause particle resuspension and local enrichment. The particle velocity characteristics are highly consistent with the gas-phase flow field analysis results.

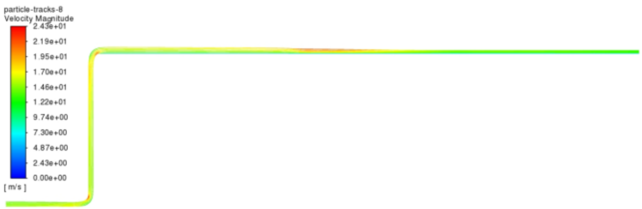

Figure 10. Particle velocity distribution

The particle density distribution reflects the spatial distribution of dust and how reactions and flow affect it. The particle density is uniformly distributed in the inlet and upstream areas, but decreases markedly in the middle horizontal pipe section, corresponding well to the gas-phase low-density zones. This is attributed to three factors: (1) the high-temperature environment causes thermal expansion of gas around particles, and reactions shorten the residence time of local particles; (2) the coupling between particles and gas phase is intensified; (3) particles are transported rapidly with high-speed gas flow. Particle density tends to remain stable in downstream areas, where particles mainly flow with the reaction products.

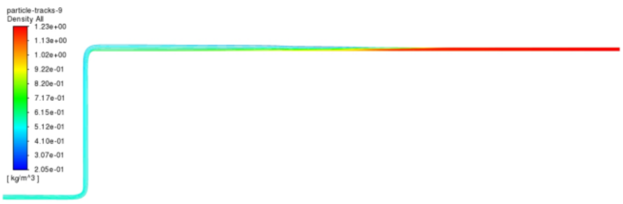

Figure 11. Particle density distribution

4. RECOMMENDATIONS FOR SAFETY MANAGEMENT AND CONTROL MEASURES

Based on the deflagration mechanism and the distribution characteristics of hazardous areas revealed by numerical simulation, targeted measures are proposed to reduce deflagration risks in the ventilation and dust collection system in polyimide foam production lines and improve the plant's intrinsic safety level.

(1) Optimize duct structure and strengthen protection for key parts: Simulation results show that duct elbows and the middle horizontal section are areas with the most intensive coupling of flow, reaction, and pressure, which should be prioritized for protection in engineering design and renovation. For elbows, a larger curvature radius is recommended to reduce flow separation and pressure concentration. Meanwhile, improve the pressure and impact resistance of the above pipe sections, and install explosion-proof reinforcement or explosion-resistant liners when necessary.

(2) Reasonably configure explosion venting and isolation facilities: To cope with local overpressure caused by deflagration, explosion venting devices such as rupture discs and explosion relief valves should be properly arranged in high-risk areas to release pressure rapidly under abnormal conditions. In addition, explosion isolation devices should be installed at appropriate positions to block the propagation of flames and pressure waves along the duct and prevent accidents from spreading upstream and downstream.

(3) Strengthen control over dust concentration and combustible gases: Source control is the most effective means to eliminate explosion risks [20]. Optimize process parameters and ventilation & dust removal efficiency to strictly control polyimide dust concentration inside the duct and keep it permanently below the lower explosion limit. Meanwhile, monitoring and control of combustible gas leakage and accumulation should be enhanced to avoid high-risk conditions from coexisting combustible gas and dust.

(4) Establish an online monitoring system for temperature, pressure, and species: Based on the identification of high-temperature zones and pressure-sensitive areas, a multi-point online monitoring system should be deployed to realize real-time monitoring of temperature, pressure, and concentration of key species. The system should send timely alarms and trigger an interlock shutdown when abnormal parameter increases are detected, to eliminate hazardous conditions before deflagration occurs.

(5) Control ignition sources and operational disturbances: Potential ignition sources in high-risk areas should be strictly managed to prevent ignition caused by static accumulation, mechanical friction, and high-temperature surfaces. Avoid frequent start-stop operations and drastic fluctuations in working conditions during production to reduce sudden changes in flow and pressure and lower the probability of deflagration.

(6) Improve safety management and emergency response capabilities: On the basis of engineering measures, safety management systems and emergency plans should be improved synchronously. Regular inspection of ventilation and dust removal systems, special risk assessment on dust explosions, and emergency drills should be carried out to improve staff's ability to identify deflagration risks and handle emergencies. A multi-level safety protection system combining engineering control and management control should be established.

5. Conclusion

Using the ventilation and dust-collection duct of a polyimide foam production line as the research object, this paper establishes a numerical deflagration model using Fluent and simulates and analyzes the propagation of combustible-media deflagration inside the duct. The paper studies the flow field, temperature field, pressure field, species distribution, and particle-phase motion characteristics, and discusses the formation mechanism of hazardous areas. The main conclusions are as follows:

(1) The velocity field inside the duct presents obvious spatial inhomogeneity. High-speed flow occurs at elbow sections and areas with structural discontinuities. Changes in flow direction and local cross-section variation increase turbulence intensity, promote re-suspension and local enrichment of polyimide dust particles, and provide favorable dynamic conditions for deflagration propagation.

(2) The middle horizontal section of the duct forms a distinct high-temperature and low-density zone, which is the primary deflagration reaction area. The peak gas temperature in this zone reaches approximately 1680 K, and the minimum gas density drops to 0.20–0.40 kg/m³. Intense exothermic reactions occur in this area, where combustible media are rapidly consumed, and gas expands significantly.

(3) Obvious pressure concentration occurs at elbow sections due to geometric constraints and the superposition of reflected pressure waves. Although the overall absolute pressure is close to ambient pressure under the simulated condition, local pressure rise at elbows indicates that these areas are highly sensitive to deflagration shock waves, and dangerous overpressure peaks are likely to form under adverse conditions such as higher dust concentration or localized confinement.

(4) Species distribution results confirm that methanol and oxygen are rapidly consumed in the middle horizontal section, accompanied by massive CO_2 generation, which further verifies that this area is the main reaction zone. Particle phase analysis shows significant momentum and energy coupling between polyimide dust particles and the gas phase. Particles are prone to collision, deposition and local aggregation at elbows, which increases the risk of deflagration propagation.

(5) Elbow sections and local structural discontinuities are identified as the critical hazardous areas of the ventilation and dust removal system. Targeted prevention and control measures, including duct structure optimization, explosion venting and isolation design, dust concentration control, and online monitoring system improvement, are proposed to improve the overall safety level of the production line.

Ethical issue

The authors are aware of and comply with best practices in publication ethics, specifically with regard to authorship (avoidance of guest authorship), dual submission, manipulation of figures, competing interests, and compliance with policies on research ethics. The authors adhere to publication requirements that the submitted work is original and has not been published elsewhere.

Data availability statement

The manuscript contains all the data. However, more data will be available upon request from the corresponding author.

Conflict of interest

The authors declare no potential conflict of interest.

References

[1] Yang F K, Zhang Y D, Deng Y Y, et al. Research Summary on Properties of Polyimide Foam Materials. China Plastics, 2020, 34(11): 94-101.

[2] Wu H T, Liu T T, Pan L, et al. Research and Application of Polyimide Foam. New Chemical Materials, 2023, 51(10): 231-234+238.

[3] Li J W, Zhang G C, et al. Synthesis and Properties of Polyimide Foams Containing Benzimidazole Units. RSC Advances,2016,6(65):60094-60100.

[4] Zhan M S, Wang K. Polyimide Foam[M]. Beijing: National Defense Industry Press, 2010. ISBN: 978-7118067231

[5] Sun G H, Zhang X, Wu D Z, et al. Research Progress of High-performance Polyimide Composites. China Plastics, 2021, 35(09): 147-155.

[6] Zhang Y D, Yu H, Xu X Y. Research Progress of Inorganic Material Modified Polyimide Composites. Synthetic Resin and Plastics, 2021, 38(3): 71-76.

[7] Li R H, Bao Y, Zhao H H. Research progress of polyimide composite thermal insulation materials. Materials Reports, 2025, 39(10): 231-240.

[8] Ma J J, Xiong C X, Jiu Y B, et al. Structure and Properties of Ultra-light Polyimide Foam Prepared by Powder Microwave Foaming Method. Polymer Materials Science & Engineering, 2019, 35(06): 66-72+78.

[9] Su B, Dong H W, Luo Z M, et al. Research Progress on Dynamic Characteristics and Mechanism of Gas-dust Two-phase Explosion. CIESC Journal, 2024, 75(06): 2109-2122.

[10] Jia J L, Sun Y L, Zhou H F, et al. Preparation and Properties of Polyimide Foam by Powder Method. New Chemical Materials, 2025, 53(03): 88-91.

[11] Wang N, Li C F, Liu M L. Research Progress and Application of Modified Melamine Formaldehyde Resin. Thermosetting Resin, 2020, 35(6): 62-65.

[12] Ya B, Ding Z J, Pei L, et al. Properties and Microstructure of High-strength Composite Foam Modified by Polyimide Particles. Plastics Science and Technology, 2025, 53(09): 1-7.

[13] Xu Y, Wang Y D, Xu H, et al. Design of High-resilience Silicone-modified Polyimide Foam Materials. Aerospace Materials & Technology, 2024, 54(06): 59-64.

[14] Safonov A. N.,Kornienko P. V.,and Shirshin K. V..Preparation of a Structural Polyimide Foam Plastic Based on a Bulk Copolymer of Acrylonitrile and Methacrylic Acid. Russian Journal of Applied Chemistry,2024,96(4):468-473.

[15] He Q L. Brief Analysis on the Role of Numerical Simulation Software Fluent in Coal Mine Gas Explosion. Green Science and Technology, 2014(03): 127-128.

[16] Fang Y, Mei J, Zhang H, et al. Numerical simulation study of the effect of coal dust on gas explosion overpressure. Scientific Reports, 2025, 15(1): 35254.

[17] Singha A K, Roy A, Singh A K. Numerical Investigation of Mixed Convection Flows with Variable Viscosity and Prandtl Number and Validation Using ANSYS FLUENT. Journal of Applied & Computational Mathematics, 2021, 10(3): 1-6.

[18] Bae Y Y. Computation of Upward Pipe Flows at Supercritical Pressures with Blended Turbulence Model. International Journal of Heat and Mass Transfer,2021,168: 68-73.

[19] Song Y ,Zhang Q ,Wang B , et al. Numerical study on the internal and external flow field of dust explosion venting. International Journal of Thermal Sciences,2019,145: 106008.

[20] Li H, Wang T, Lu K. Hidden Danger Analysis and Risk Control of Enterprises Involved with Dust Explosion. Industrial Safety and Environmental Protection, 2020, 46(02): 41-43.